HEAT AND MASS TRANSFER BETWEEN SOIL AND ATMOSPHERE: HANNO CASE STUDY

Pham Hong SON[1] and Kuniaki SATO[2]

[1] Member of JSCE, Hydroscience and Geotechnology Lab., Saitama University (255-Shimo-Okubo, Urawa, Saitama 338-8570, Japan)

[2] Member of JSCE, Prof. Dr. Hydroscience and Geotechnology Lab.,Saitama University, (255-Shimo-Okubo, Urawa, Saitama 338-8570, Japan)

This study concerns with an integrated simulation of coupled heat and mass transfer between soil and atmosphere. A model is constructed in one-dimension from ground water table up to upper atmospheric boundary layer. Numerical solutions of momentum, heat and mass transport equations are available for prediction of physical processes occurring in atmospheric boundary layer and in porous bodies. The processes in the atmosphere and in the porous bodies are linked each other through the equations of heat and mass conservation. The water mass in the soil is treated as a two-phase mixture of liquid water and vapour. The simulated results are supported by the observation data recorded with a meteorological station placed in the experimental field in Hanno new resident town, Saitama prefecture. A good agreement indicates that the model is reliable for predicting a water budget dynamics in a zone near ground surface and atmosphere.

***Key Words**: Coupled Heat and Mass, Evaporation, Unsaturated Flow*

1. INTRODUCTION

Evaporation is an important element in hydrological cycle and has been studied by both geohydrologists and meteorologists. Traditionally, geohydrologists concentrate in mass and heat transfer in capillary porous bodies from groundwater table up to soil surface while meteorologists focus on physical processes occurring in and above the surface boundary layer. The surface is considered mostly as boundary condition in each of their studies.

Land surface is a hydrologic layer, through which the heat and mass transfer between soil and atmosphere occur. The transfer processes depend on both soil surface layer and atmospheric surface layer as well as surface conditions. Land use, or surface condition are responsible for partitioning of heat fluxes which drive the evaporation process. Accompanying with atmospheric surface condition, it plays a significant role in momentum exchange in surface layer. Available of the moisture at the soil surface, heat and mass transport in capillary porous bodies are also important factors in evaporation process[1,2].

Several well-posed tasks of computing evaporation from soil have been bypassed in many numerical models of the atmosphere by specifying some measures of the surface wetness. These kinds of model normally required many parameters and physical properties. For some purposes this may acceptable, but it is a very crude representation of the evaporation process and in particular, fails to include properly the feedback between the atmosphere and surface moisture status. Therefore, it is useful to consider soil-surface-atmosphere as an integrated system.

SALSA (Soil Atmosphere Linking Simulation Algorithm) (ten Berge[3] 1990) is one of energetic models to overcome this drawback. Following this algorithm, the heat and mass transfer between soil and atmosphere in Hanno test site was simulated to investigate the local hydrological characteristics.

2. METHODOLOGY OF COMPUTATION

The modified model in the study is composed of three main parts: surface, atmospheric and soil with equations of mass and energy conservation. For the sake of simplicity, it is assumed that the domain concerned is homogeneous in the horizon. Using measured meteorological data and surface conditions, the model can estimate the heat and mass transfer between soil and atmosphere through the soil surface. After that, the physical processes occurring in the atmospheric boundary layer and porous media are simulated. Only main

methodology of the model is described in this study.

(2.1) Atmosphere modelling

The equations describing momentum, temperature and moisture in vertical direction are simplified in the following forms (ten Berge[3] 1990):

$$\frac{\partial u}{\partial t} = f\left(v - v_g\right) - \frac{\partial}{\partial z}\frac{\tau_x}{\rho}, \tag{1}$$

$$\frac{\partial v}{\partial t} = -f\left(u - u_g\right) - \frac{\partial}{\partial z}\frac{\tau_y}{\rho} \tag{2}$$

$$\frac{\partial \theta}{\partial t} = -\frac{\partial}{\partial z}\left(\frac{H}{\rho C_p}\right) \tag{3}$$

$$\frac{\partial q}{\partial t} = \frac{\partial}{\partial z}\left(\frac{E}{\rho}\right) \tag{4}$$

where u, v are the two components of horizontal velocity, u_g, v_g the corresponding geostrophic velocities, f the Coriolis parameter, ρ the air density, q the moisture mixing ratio (kg water/kg dry air), H the sensible heat flux, E the vapour flux (kgm^{-2}s^{-1}), θ the potential temperature, C_p the specific heat of air and τ the shear stress.

Momentum, sensible heat and vapour flux transport can be written using eddy diffusivities $K_{M,H,V}$ as follows:

$$\tau_x = -\rho K_M \frac{\partial u}{\partial z}, \quad \tau_y = -\rho K_M \frac{\partial v}{\partial z} \tag{5}$$

$$H = -\rho C_p K_H \frac{\partial \theta}{\partial z}, E = -\rho K_V \frac{\partial q}{\partial z} \tag{6}$$

where the subscripts M,H and V denote moment, heat and vapour, respectively. The constant vertical fluxes are given by

$$K_{M,H,V} = l_{M,H,V}(Ce)^{0.5}. \tag{7}$$

The length scales $l_{M,H,V}$ are computed from similarity functions $\phi_{M,H,V}$

$$l_{M,H,V}^{-1} = \frac{\phi_{M,H,V}(\zeta)}{\kappa z} + \frac{f}{\alpha u_g} \tag{8}$$

in which stability parameter $\zeta = z/L$, L is Monin-Obukhov length scale, κ the Karman constant, α and C the empirical coefficients equal 4×10^{-4} and 0.2, respectively. The above system is closed by the turbulent kinematic energy e (TKE) equation (Tennekes & Lumley[4] 1972)

$$\frac{\partial e}{\partial t} = \frac{\tau_x}{\rho}\frac{\partial u}{\partial z} + \frac{\tau_y}{\rho}\frac{\partial v}{\partial z} + \frac{g}{T}\frac{H}{\rho C_p} + \frac{\partial}{\partial z}K_M\frac{\partial e}{\partial z} - \frac{(ce)^{3/2}}{l_M} \tag{9}$$

where T is air temperature (K).

For the atmospheric surface layer, the velocity and potential temperature are determined by following equations

$$u = \frac{u_*}{\kappa}\left(\ln\frac{z}{z_{o,M}} - \psi_M\right), \tag{10}$$

$$\theta = \theta_o + \frac{\theta_*}{\kappa}\left(\ln\frac{z}{z_{o,H}} - \psi_H\right) \tag{11}$$

where θ_o is extrapolated temperature to roughness parameter z_o and * denotes the friction values of the corresponding properties. The functions ψ are determined from Paulson[10] (1970) and Businger[11] (1975) which are cited in ten Berge[3] (1990).

(2.2) Heat and water transfer in soil.

The problem of unsaturated flow induced by evaporation and integrated coupling of heat and mass has been discussed in many studies (Philip & de Vries[5], Milly[1], Tzimopoulos[6], Fukuhara[7] et al. The equation used for describing the heat transfer in capillary porous bodies is simplified in the form:

$$C_s\frac{\partial T_s}{\partial t} = \frac{\partial}{\partial z}\left(\lambda\frac{\partial T_s}{\partial z} + J_v H_v\right) \tag{12}$$

where T_s is the soil temperature, J_v (kg m^{-2}s^{-1}) the vapour flux and H_v (Jkg^{-1}) the latent heat of water vaporisation. The soil capacity C_s (Jm^{-3}K^{-1}) and the soil conductivity λ (Wm^{-1}K^{-1}) are determined from volumetric participants f_i of porous body as followings

$$C_s = \sum_i f_i C_i \tag{13}$$

$$\lambda = \frac{\sum_i f_i \lambda_i k_i}{\sum_i k_i f_i} \tag{14}$$

where C_i, λ_i are the heat capacity and the conductivity of porous media elements and k_i the weighting factors for heat conductivity of porous media elements.

The water in the soil is treated here as a two-phase mixture of liquid water and water vapour. The liquid water equation is given in the form:

$$\rho_l\frac{\partial \theta_w}{\partial t} = \frac{\partial}{\partial z}\left[K(\theta_w, T_s)\frac{\partial p(\theta_w, T_s)}{\partial z}\right] - \rho_l g\frac{\partial}{\partial z}K(\theta_w, T_s) \tag{15}$$

where p is the potential pressure (Pa), K the hydraulic conductivity (kgm^{-1}Pa^{-1}s^{-1}), ρ_l the ground water density, g the gravity acceleration and θ_w the volumetric water content.

The water vapour transfer is expressed by

$$\rho_l \frac{\partial \theta_v}{\partial t} = \frac{\partial}{\partial z}\left[D(\theta_v, T_s) \frac{\partial \rho_v(\theta_v, T_s)}{\partial z} \right] \qquad (16)$$

where ρ_v is the vapour density (kgm^{-3}), θ_v the volumetric vapour content, D the diffusion coefficient of vapour m^{2}s^{-1}. To solve equations (12), (15) and (16), it is required to know K, ρ_v and D as functions of the local soil temperature and the water content which describe the coupling of particular event with others. Among alternative available equations, Van Genuchten's[8] equation for hydraulic conductivity, the well-known approach of Philip and de Vries[5] (1957) for ρ_v and of Cary[9] (1963) for D are used herein. Details of the analyses are given in ten Berge[3] 1990.

(2.3) Mass and heat conservation at the surface

Computational algorithm in soil is linked with that in the atmospheric by the surface condition where the conservation of heat and water mass is specified. It is assumed that there is no storage of heat and mass on surface layer. The net radiation is divided into sensible, latent and ground heat fluxes, which are the condition for solving equations in both porous body and atmospheric boundary layer. The water mass transfer through the surface is composed of evaporation from soil and precipitation.

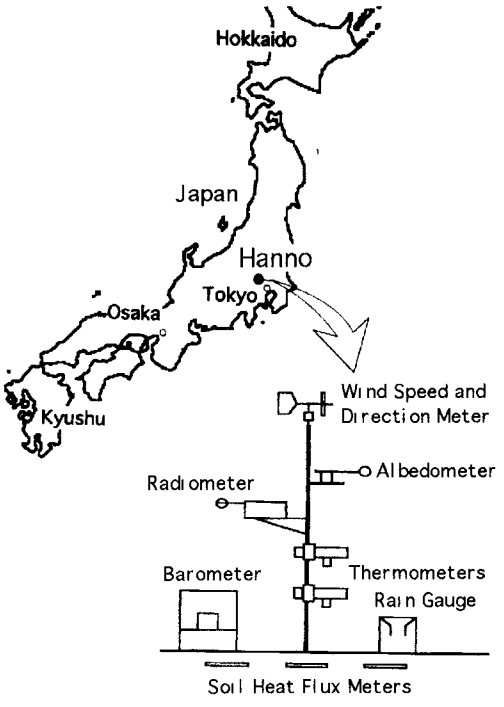

Fig.1 Location of observation field and system of measurement

3. OBSERVATION FIELD SITE

The field site where the measurement system is stationed is located in Hanno new resident town, Saitama prefecture (35°53'N, 138°36'E) (see Fig. 1). The geology of the site consists of an alluvium above a basement in the Mesozoic and Paleozoic era, and the upper layer is covered with the talus, river deposits and unconsolidated gravel. The original topography of the project site is mountainous, and the gradient of slope in valleys is steep ranging from 30 to 40 degrees. The permeability of the site is small because the formation of mountain is composed of weakly cemented gravel. At present, a large-scale land development is under way. Under the plan, a total 137.7 hectare of natural forest will be removed and a new resident city will be build with 30% area for resident complex, 26% for public facilities and the rest for transportation and green area. To predict the local thermal and hydrological characteristics, the observation and numerical study have been carried out.

The meteorological variables: air temperatures at two heights (0.5 and 1.0m), humidity (wet- and dry-bulb), solar radiation, ground heat flux, albedo, precipitation, atmospheric pressure, wind speed and direction, have been measured at every minute. In addition to the meteorological observation, the soil samples are taken at every 5cm from surface down to 1m deep on Aug. 12, 1997 to identify the soil hydraulic properties, its geological structure and the water content with laboratory experiments. Also on this day the thermal sensors were installed to record the soil temperature at corresponding depth.

4. SIMULATION RESULTS

(4.1) Simulation condition

The simulation is carried out for a selected domain from groundwater table up to 1500 m in atmospheric boundary layer with an assumption that the domain is considered horizontally homogeneous. The groundwater table is fixed at 1.5m below the ground surface. At this boundary, the soil temperature and water content were kept constant during total simulation period. The porous body is divided into 25 layers by nonuniform computing meshes. The grid size is smallest (0.2cm) at layer nearest to the surface and gradually increases to 30cm within the groundwater table layer.

For the atmospheric computational domain,

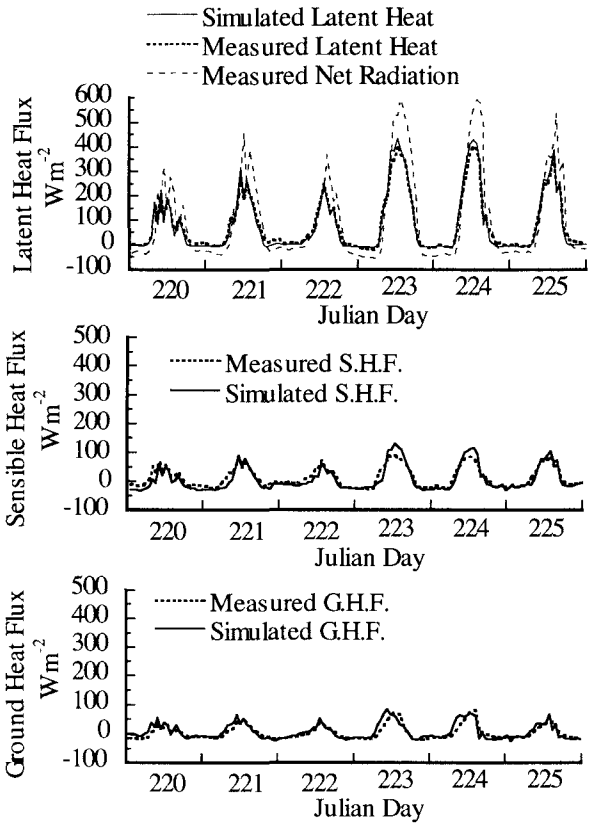

Fig.2 Surface heat fluxes: measured net radiation, latent heat flux, sensible heat flux and ground heat flux.

total 20 grid points are adopted with smallest size 1.0m at the surface and 350m for the top layer. At the top atmospheric layer, $u=u_g$, $v=v_g=0$, $\tau_x=\tau_y=0$, $H=0$, $E=0$, $\partial e / \partial z = 0$ are assumed.

The simulation was performed under condition on the field during the period Aug. 6-12, 1997, starting at 0.00 o'clock on Aug. 6. Time step is 1sec. during computational period and an implicit Crank-Nicholson difference scheme is used. The net radiation (see Fig. 2) was given during the calculation. The measured temperature and vapour mixing ratio at 1m height are also referenced. Selection of simulation period with strong solar radiation is aimed at obtaining a large range of variation in surface properties.

(4.2) Results

For each time step, the surface subroutine is called first to calculate the surface heat fluxes and surface soil temperature by solving the heat balance equation. The simulated sensible heat flux, latent heat flux and ground heat flux at surface are showed in Fig. 2 together with their observed values.

After that the system of heat, liquid water and water vapour transfer equations in porous body is solved. Identification of soil properties of collected samples shows that the soil in the experiment site has

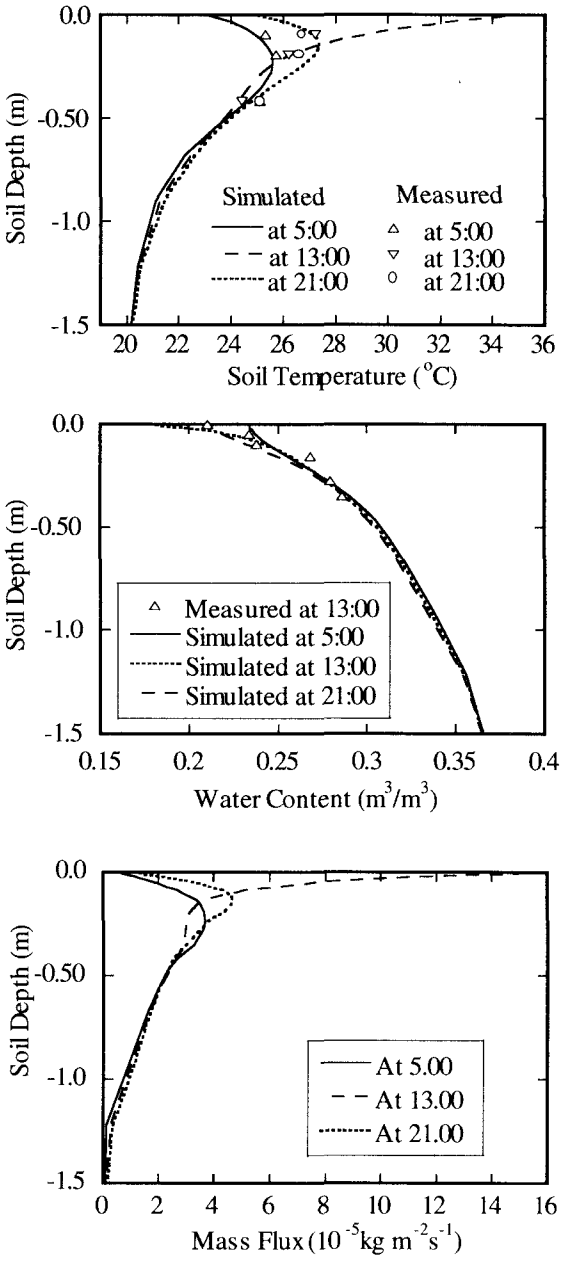

Fig.3 Simulated profiles of soil temperature, water content and mass flux in soil below ground on Aug. 12, 1997

nearly homogeneous structure and parameters from surface down to 0.7m. In the lower zone the soil structure becomes more complicated because of being mixed with gravel. The average value of the soil properties in near ground surface is used herein.

Fig. 3 shows the simulated profiles of the soil temperature, the water content and the water mass flux from ground water table toward the surface on Aug. 12 (Julian day 225) at 5:00, 13:00 and 21:00 o'clock. On this day, the net radiation at noon was very strong (see Fig. 2). As a result, the variation of

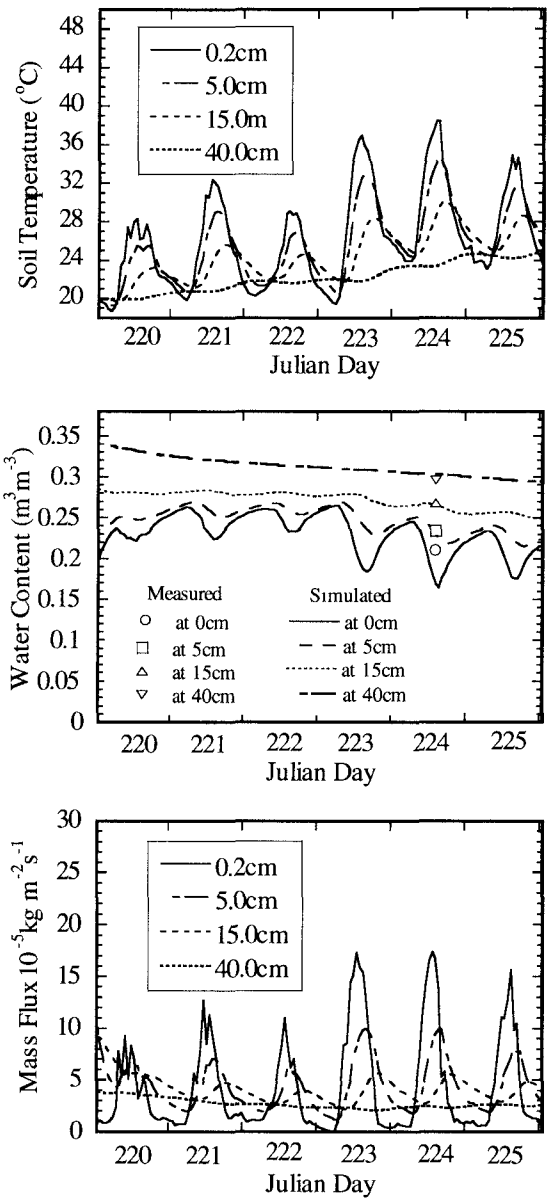

Fig. 4 Time dependence of simulated soil temperature, water content and mass flux at several ground depths

heat and water mass can be clearly observed on upper part of porous domain (0-0.5m deep). On the other hand these variations are smaller in lower layers. This characteristic can be seen in the Figure 4, the plots of soil temperature, water content and water mass flux at 0.2, 5.0, 15.0 and 40.0 cm deep with time.

The absent of precipitation during the simulated period causes the surface to be drying, especially for the last two days when the input of net radiation is very strong. Evaporation in reality will appear in an interface layer near the surface of the soil, which lowers capillary zone and creates upper drying zone. A large amount of water in the capillary zone is in liquid phase while in drying zone it is in vapour phase.

It can be found that, the development of drying zone in the near ground surface during daytime accelerates the temperature change while a thermally induced mass flow plays an important part in moisture deficit by evaporation. In addition to the capillary flow, the thermally induced flow caused by a sharp gradient of temperature contributes to recharging of water in near ground zone.

Before completing the time step, the system of atmospheric equations is solved. The profiles of simulated air potential temperature, mixing ratio and horizontal velocity on Aug. 12 at 5:00, 13:00 and 21:00 o'clock are demonstrated in the Fig. 5. Their temporal variations at 1.0 m, 20 m, and 380m during the simulated period are plotted in the Fig. 6. It is clear that the diurnal air temperature in the layer lower than 800 m is strongly changes while in the layer higher than 800 m weaker effect is observed. As a result of evaporation from the surface, the vapour in the atmospheric surface layer increases at noon. This vapour is convected upward due to turbulent eddies which are caused by buoyancy and momentum transfer. The simulated results provide the understanding of the heat and water mass variation in lower atmospheric layer

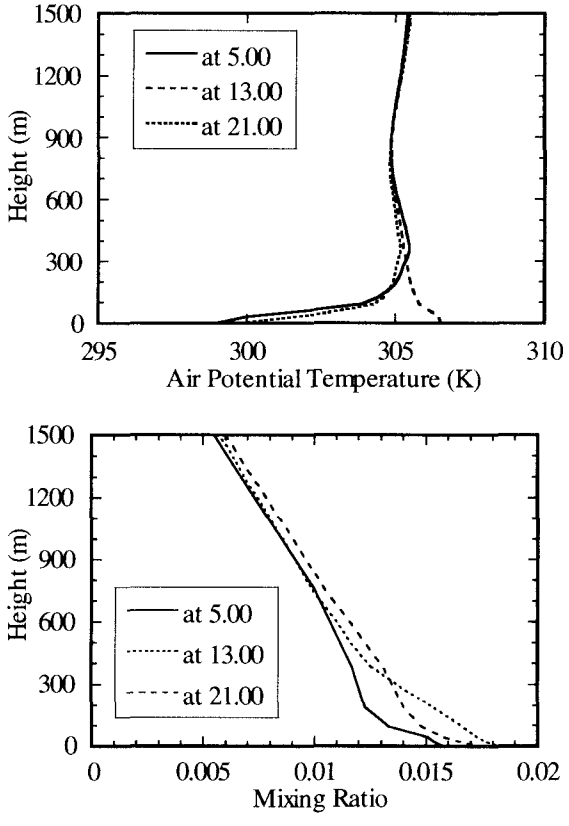

Fig.5. Simulated profiles of air potential temperature, and mixing ratio with time on Aug. 12. 1997

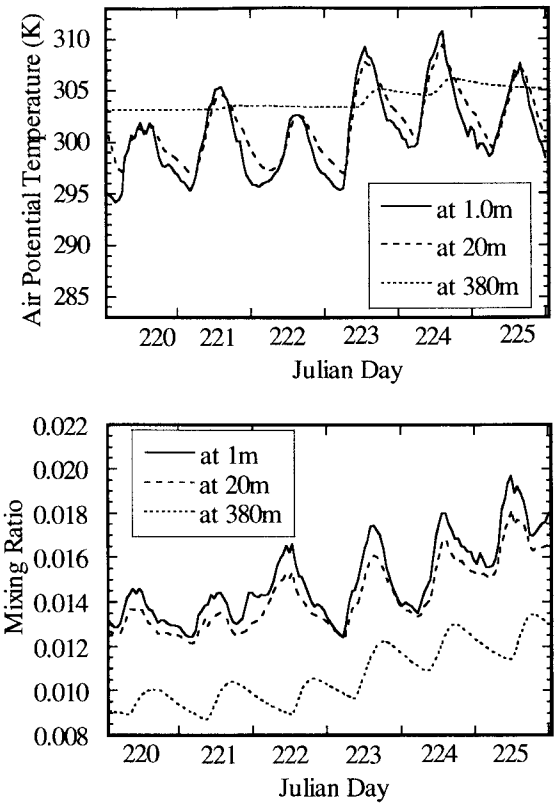

Fig.6 Time dependence of simulated air potential temperature and mixing ratio at several heights.

and soil. However, the atmospheric algorithm is constructed in one dimension that may lead to some deviations of computed results from reality. Although the experimental field was well arranged, the nearby hills might cause significant horizontal variations in momentum, heat or vapour transfer processes. Another reason could be the lack of initial profiles of upper atmospheric layer.

5. CONCLUSION

The obtained results indicate that the model successfully describes the physical heat and mass transfer in the computational domain from groundwater table up to upper boundary layer. The model therefore will be useful as a predicting tool for estimation of evaporation from soil.

The simulation process has proved that an accuracy of the model depends on a set of local characteristics: soil structure, its conductivity and surface roughness.

Dependency between variables in porous bodies is prejudiced and exhibits that requires appropriate numerical algorithm for solving a set of differential equations. Special attention should be given to capillary force resulting in saturation and thermal induced effects, molecular diffusion due to local vapour pressure and gravity.

ACKNOWLEDGEMENT: The authors would like to express their appreciation to the Housing Urban Development Corporation for providing the research data

REFERENCES

1. Milly P.C.D., Unsaturated flow induced by evaporation and transpiration, *Unsaturated Flow in Hydrologic Modelling. Theory and Practice*, H.J. Morel-Seytoux Eds., Kluwer Academic Publishers, pp.221-240, 1989.
2. Bories, M. Recan, K. Sato & T. Fukuhara, Simulation of heat and mass transfer between bare soil and atmosphere, *Annual J. of Hyd. Eng. JSCE*, Vol. 36, pp.459-464, 1992.
3. H.F.M. ten Berge, Heat and water transfer in bare topsoil and the lower atmosphere, Centre for Agricultural Publishing and Documentation (Pudoc) Wageningen, the Netherlands, 1990.
4. Tennekes H. & Lumley J.L., *A first course in turbulence.* The MIT Press, Cambridge, Massachusetts, 1972.
5. Philip & de Vries, Moisture movement in porous materials under temperature gradients. *Transactions of the American Geophysical Union* 38: pp.222-231, 1957.
6. Tzimopoulos C. & Sidiropoulos E., Coupled heat and moisture transfer in unsaturated porous bodies, *Flow and Transport in Porous Media*, A. Verruijt & F.B.J. Barends, Eds., A.A. Balkema Rotterdam, pp.169-172, 1981.
7. Fukuhara T., G.F. Pinder & Sato K. An approach to fully coupled heat and moisture transfer analysis in saturated unsaturated porous media during surface evaporation, *Proc. of Japan Society for Civil Engineers* (JSCE) Vol. 423/II-14 pp 111-120, 1990.
8. Rawls W.J. & Brakensiek D.L., Estimation of soil water retention and hydraulic properties, *Unsaturated Flow in Hydrologic Modelling. Theory and Practice*, H.J. Morel-Seytoux Eds. pp. 275-300, 1989.
9. Cary J.W., Soil heat tranducers and water vapor flow, *Soil Science Society of America Journal* 43: pp.835-839, 1979.
10. Paulson C.A., The mathematical representation of windspeed and temperature profiles in the unstable atmospheric surface layer. *Journal of Applied Meteorology* 9, pp.857-861, 1970.
11. Businger J.A., Aerodynamics of vegetated surfaces, *Heat and Mass Transfer in the Biosphere.* D.A. de Vries & N.H. Afgan. Scripta Eds. Wash D.C. pp.139-167, 1975.

(Received September 30,1998)